J. Fluid Mech. (1985), *vol.* 154, *pp.* 29–42
Printed in Great Britain

Torque measurements on a stationary axially positioned sphere partially and fully submerged beneath the free surface of a slowly rotating viscous fluid

By J. G. KUNESH,
Fractionation Research Inc., 1517 Fair Oaks Ave., South Pasadena, CA 91030

H. BRENNER,
Department of Chemical Engineering, Massachusetts Institute of Technology, Cambridge, MA 02139

M. E. O'NEILL
Department of Mathematics, University College, London WC1E 6BT

AND A. FALADE
Department of Mechanical Engineering, University of Lagos, Lagos

(Received 21 February 1984 and in revised form 9 November 1984)

Experimental measurements are presented for the hydrodynamic torque exerted on a stationary sphere situated at the axis of a slowly rotating viscous liquid at small rotary sphere Reynolds numbers ($Re < 0.1$) as a function of depth of submersion of the sphere below the free surface. Effects of free-surface proximity on the torque furnished the impetus for the study. Experiments were performed for different depths of sphere immersion beneath the free surface, varying from full to partial submersion. Rotation rates were maintained sufficiently low to approximate a planar interface. Torque measurements agreed well with existing theoretical predictions for both the interface-straddling and fully submerged sphere cases. In particular, the predicted continuity of the torque and its derivative at the interface-penetration point (where the sphere first starts to protrude through the free surface) was observed. Free-surface curvature as well as meniscus-curvature effects upon the torque were found to be negligible in the experiments, including even the extreme case where the sphere was in the almost fully withdrawn configuration.

1. Introduction

Rotating-sphere and falling-ball viscometers (Walters & Waters 1963; Ashare, Bird & Lescarboura 1965; Geils 1977; Cho & Hartnett 1979; Fluide & Daborn 1982) utilize theories of the hydrodynamic resistance of rotating and translating spheres immersed in fluids whose rheological properties are sought. The most widely used of these theories pertains to motion in unbounded fluids under various dynamical and kinematical conditions. This paper has as its objective the presentation of experimental results obtained for the hydrodynamic torque engendered by the relative rotation of a sphere in proximity to the free surface of a Newtonian liquid, and the comparison of these torque measurements with existing theory.

Kirchhoff (cf. Lamb 1932) derived his well-known expression for the torque

$$T_\infty = 8\pi\mu a^3\Omega \tag{1}$$

on a sphere of radius a rotating at angular velocity Ω in a fluid of viscosity μ. This expression applies at small rotary Reynolds numbers $Re = a^2\Omega\rho/\mu \ll 1$. Corresponding results for elastico–viscous fluids were obtained by Thomas & Walters (1964) and Wein (1979) for a rotating sphere, and by Waters & Gooden (1980) for a rotating oblate spheroid. Dennis, Singh & Ingham (1980) give Newtonian-fluid solutions for rotating spheres in the low- and moderate-Reynolds-number range, where inertial effects are sensible. Their results for the range $10 < Re < 100$ are in excellent agreement with the experimental data of Sawatzki (1970). Dennis & Ingham (1982) obtained solutions valid in the range $Re > 5000$. Velocity fields predicted by their analysis show qualitative agreement with the experimental results of Bowden & Lord (1963) at locations in proximity to the sphere, and to those of Richardson (1976) at large distances.

Theoretical analyses are also available (Childress 1964; Dennis, Ingham & Singh 1982) for the slow translational motion of a sphere in a rotating fluid. Dennis *et al.* (1982) report favourable agreement between their results and the experiments of Maxworthy (1965). Equally worthy of note in this context are the experimental investigations of Taylor (1923), Davis (1965) and Maxworthy (1970).

Theories have also been proposed for establishing boundary-proximity effects upon bodies rotating and/or translating at small Reynolds numbers near rigid container walls (Brenner 1964*a*; Sonshine *et al.* 1966; Cox & Brenner 1967*a*; Hocking, Moore & Walton 1979; Munro, Piermarini & Block 1979; Hirschfeld, Brenner & Falade 1984 for Newtonian fluids; Caswell 1970 for non-Newtonian fluids), as well as near free surfaces (Brenner 1964*a*; Kunesh 1971; Davis & O'Neill 1979) and interfaces separating immiscible fluids (Schneider, O'Neill & Brenner 1973; Majumdar, O'Neill & Brenner 1974; Ranger 1978; Leal & Lee 1982, O'Neill & Ranger 1979; Falade 1982). These studies point to the existence of substantial deviations from unbounded-fluid behaviour arising from the presence of boundaries nearby to the sphere.

Attempts to improve upon the accuracy of viscometers of the types earlier described must contend with ever-present wall and/or free-surface effects. The confidence with which theoretically derived boundary-effect calculations of hydrodynamic resistance may be employed to extrapolate these data to unbounded fluids is obviously enhanced by experimental confirmation of these purely theoretical predictions. Few such studies exist for cases of rotary motion (Mena, Levinson & Caswell 1972), and none of which we are aware pertain to motion near a free surface. This dearth of data furnished part of the motivation behind the present study – which was in fact originally conceived (Kunesh 1971) in the broader context of experimentally studying low-Reynolds-number hydrodynamic 'coupling' (Brenner 1964*b*) between translational and rotational motions of asymmetric particles.

In addition to the viscometric emphasis cited above, much interest currently exists in the molecular modelling of interfacial transport processes. A recently proposed model (Brenner & Leal 1978, 1982) involves a spherical Brownian particle moving in proximity to, and straddling, a non-deformed interface separating two immiscible fluids. That theory depends critically upon knowledge of the Stokes resistance of the particle in relation to its motion at and near the interface. In this context our experiments represent an additional contribution (Leal & Lee 1982; Berdan & Leal 1984) towards further understanding of the hydrodynamic aspect of the interfacial transport phenomena.

Explicitly, the present paper summarizes the results of experiments performed to measure the viscous torque exerted on a stationary sphere present in a rotating fluid bounded by an effectively planar free surface at small Reynolds numbers ($Re < 0.1$). A brief summary of the contents of this paper is as follows. Relevant theoretical results are briefly reviewed in §2, where the fluid-mechanical equivalence of the stationary-sphere–rotating-fluid arrangement to that of the rotating-sphere–stationary-fluid case is pointed out (at least to the extent that centrifugal/inertial forces are negligible, so that the free surface remains planar). Section 3 provides a description of the apparatus employed in the experiments. Experimental procedures are detailed in §4. Finally, §5 presents the experimental results, comparing these with the theoretical results of Jeffery (1915) and Brenner (1964*a*) for a fully submerged sphere and those of Kunesh (1971) and Schneider *et al.* (1973) for a partially submerged sphere straddling the interface.

2. Theoretical background

By a simple extension of Jeffery's (1915) bipolar coordinate solution for a sphere rotating symmetrically near a rigid plane wall, Brenner (1964*a*) and Cox & Brenner (1967*b*) derived the expression

$$\frac{T}{T_\infty} = \sinh^3\eta_0 \sum_{m=1}^{\infty} \frac{(-1)^{m+1}}{\sinh^3 m\eta_0} \tag{2}$$

for the Stokes torque T on a fully submerged sphere slowly rotating in an otherwise quiescent viscous fluid about an axis normal to a planar free surface. The parameter η_0 is defined by the expression $\cosh\eta_0 = h/a$ ($0 \leqslant \eta_0 < \infty$, $1 \leqslant h/a < \infty$), with h the distance of the sphere centre from the free surface. For $a/h \ll 1$, (2) takes the asymptotic form (Brenner 1964*a*)

$$\frac{T}{T_\infty} = 1 - \frac{1}{8}\left(\frac{a}{h}\right)^3 + O\left(\frac{a}{h}\right)^8. \tag{3}$$

In the limit it reduces to Kirchhoff's infinite-medium result (1). Observe that the torques predicted by (2) and (3) are *less* than would obtain in the absence of boundaries. This diminished resistance contrasts with comparable translational results (Brenner 1961).

The counterpart of (2) for a partially submerged sphere, obtained (Kunesh 1971; Schneider *et al.* 1973) from a toroidal coordinate solution of Stokes equations, is

$$T/T_\infty = \tfrac{1}{2}\sin^3\eta_0\, F(\eta_0), \tag{4}$$

where

$$F(\eta_0) = \int_0^\infty (1+4s^2)\frac{\cosh s(\pi-\eta_0)}{(\cosh s\pi)\,(\cosh s\eta_0)}\,\mathrm{d}s. \tag{5}$$

Here the parameter η_0 is now defined by $\cos\eta_0 = h/a$ ($\pi \geqslant \eta_0 \geqslant 0$, $-1 \leqslant h/a \leqslant 1$), with h taken to be negative when the sphere centre O lies above the free surface of the liquid and conversely. Values of the function $F(\eta_0)$, as well as $\frac{1}{2}\sin^3\eta_0\, F(\eta_0)$, are tabulated by Schneider *et al.* (1973). Limiting values of (4) of special interest are as follows:

(*a*) *sphere totally submerged and tangent to the free surface* ($h/a = 1, \eta_0 = 0$):

$$T/T_\infty = \eta(3) \equiv 0.901\,543, \tag{6}$$

with $$\eta(k) = \sum_{m=1}^{\infty} \frac{(-1)^{m+1}}{m^k}, \tag{7}$$

($k = 1, 2, 3, \ldots$), related to the Riemann zeta function (Abramowitz & Stegun 1964);

(*b*) *sphere half-submerged* ($h/a = 0, \eta_0 = \frac{1}{2}\pi$):

$$T/T_\infty = \tfrac{1}{2}; \tag{8}$$

(*c*) *sphere totally external to the liquid and tangent to the free surface* ($h/a = -1$, $\eta_0 = \pi$):

$$T/T_\infty = 0. \tag{9}$$

It is demonstrated in the Appendix that for case (*a*) the limiting torque ratio (6), derived from (4), may also be derived from (2). Thus the torque varies continuously with sphere position at the point where the submerged sphere begins to protrude through the interface, corresponding to $h = a$. Moreover, it is also shown in the Appendix that in this same limit the torque is a differentiable function of position; explicitly, at $h/a = 1$ the derivatives of T/T_∞ with respect to h/a, obtained from the disparate formulas (2) and (4) respectively, are identical.

All results cited above pertain to the case of a sphere rotating in an otherwise-quiescent fluid, whereas the reciprocal experiments reported here correspond rather to a stationary sphere in a rotating fluid. However, in the creeping-flow region, and for negligible centrifugal effects, it is easily demonstrated that only the *relative* sphere–fluid motion is pertinent. This further assumes that the paraboloidal shape of the (undisturbed) free surface, arising from the centrifugal and gravity forces, does not depart appreciably from planarity. The range of parameters selected for experimental investigation was designed to render all such secondary effects negligible.

3. Experimental apparatus

Figure 1 depicts schematically the experimental apparatus, whose main components are described below. Further details are available elsewhere (Kunesh 1971).

Cylindrical vessel. The vessel in which the experiments were performed consisted of a 30 in. (0.76 m) diameter by 4 ft (1.22 m) long transparent plastic (Plexiglas) circular cylinder of $\frac{1}{2}$ in. (1.27 cm) nominal wall thickness. Cylinder circularity was found to be a maximum of $\frac{1}{2}$ in. (1.27 cm) out of round. During the experiments the vessel was filled to a depth of about 42 in. (1.07 m) with the working fluid, whose physical properties are described in table 1. A dust cover with a small hole drilled through it capped the cylinder.

A 1 in. (2.5 cm) thick vessel support plate served adequately to support the rather large load ($\sim$ 500 kg) created by the fluid-filled cylinder. In turn, this support plate rested on a 9.75 in. (0.25 m) outer diameter thrust bearing rated at 36000 lb (16330 kg), which was held in place by a retaining ring centred with respect to the vessel support plate.

Vessel rotation was achieved by means of a 3 in. (7.6 cm) diameter hard-rubber friction wheel in contact with the underside of the vessel support plate. The friction wheel was mounted on a shaft, which was itself connected (via an 18:1 gear reducer) to the shaft of an $\frac{1}{8}$ h.p. (93.3 W) Bodine motor equipped with a variable-speed control unit.

Sphere. The sphere employed in all experiments was a 3 in. (7.6 cm) diameter nylon sphere with a manufacturer's guaranteed roundedness tolerance of $\pm 0.05\%$.

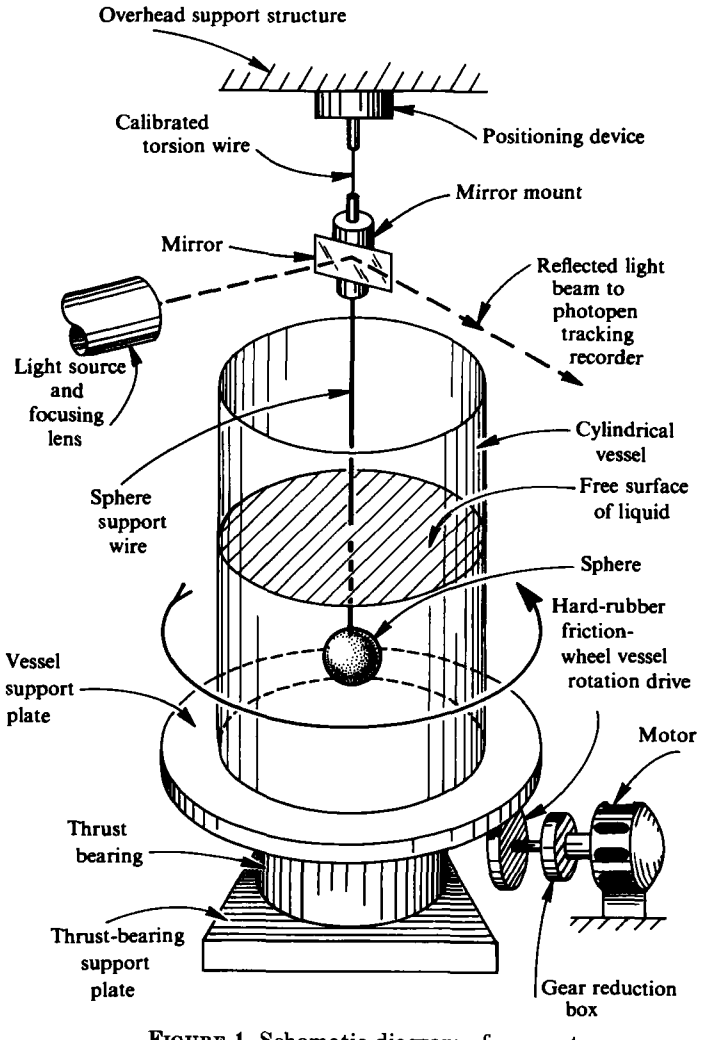

FIGURE 1. Schematic diagram of apparatus.

Temperature (°F)	Viscosity (cP)	Density (g cm^{-3})
70	6940	0.8766
72	6280	0.8760
74	5680	0.8755
76	5160	0.8749

TABLE 1. Fluid properties as a function of temperature

Permanently attached to, and embedded in, the sphere was a 0.013 in. (0.325 mm) diameter tempered-steel wire, whose imagined continuation passed through the sphere centre. This sphere–wire assembly was coupled to a torsion-measuring subsystem (situated outside of, and above, the vessel), which was rigidly attached to a structural member of the laboratory building. With the sphere fully submerged

at an effectively 'infinite' distance below the free surface, approximately 10 in. (0.25 m) of this wire was immersed in the liquid.

Alignment between the cylindrical-vessel axis and sphere centre was achieved by suspending a plumb bob from the sphere–wire coupling mechanism to a centrepunch mark in the vessel base prior to attachment of the sphere. Coincidence of the sphere centre and cylinder axis was estimated to be within several thousandths of an inch.

Torque-measuring system. Torque measurements were performed by using the 'light-lever' principle. This method, commonly employed in rheological investigations, consists in essence of reflecting a focused monofilament beam of light from a mirror mounted at the end of a calibrated torsion wire. Effectively, the linear displacement of the filament's image at a recording point located at a fixed distance from the mirror was measured and related to the angle through which the torsion wire is twisted by the action of a torque. Each of the three different torsion wires used (of nominal diameters ranging from 0.01–0.022 in. (0.25–0.56 mm)) was calibrated by measuring its period of free harmonic rotary oscillation with a disk of known moment of inertia attached to the wire – a standard procedure.

Fluid. A high-viscosity fluid was used to realize appreciable hydrodynamic torques at the relatively low fluid-rotation speeds employed to minimize centrifugal and inertial effects. Oronite polybutene 18 (Chevron Chemical Company) was used. In addition to being Newtonian and possessing viscosities in the range of interest at room temperature (table 1), this fluid is both hydrophobic and chemically stable over extended periods of time.

Considering the significant variation of viscosity with temperature (table 1), adequate temperature control was given considerable attention. This control was simply achieved by using a room air conditioner capable of maintaining temperature uniformity in the laboratory environment to within ± 1 °F cycles over 2–3 h time periods. The large fluid mass effectively insulated the liquid in the vessel from these small temperature oscillations. This fact was explicitly confirmed by temperature measurements made at various points within the liquid immediately before and after each run – in the former case after allowing a 'warm-up' period sufficient to suppress any initial transients.

3.1. *Wall-effect estimates*

First-order boundary effects upon the torque experienced by the sphere, arising respectively from the presence of the cylinder wall (radius R_0) and cylinder bottom ($h_1 \equiv$ distance of sphere centre from base) are of orders $(a/R_0)^3$ and $(a/h_1)^3$ (Brenner 1964*a*). For the experiments reported here, $a/R_0 \sim 0.10$ and $a/h_1 \sim 0.06$, leading to negligibly small wall effects of the order of one part in 10^4 – well below the limits of detection. Indeed, it was such considerations that resulted in the large size of the equipment employed in our experiments.

3.2. *Sphere-support torque correction*

The hydrodynamic torque T_w acting upon the thin wire (radius b) supporting the immersed sphere may be estimated as

$$T_w = 4\pi\mu\Omega L b^2$$

from the well-known solution (Lamb 1932) for a rotating circular cylinder. Here L is the depth of immersion of the wire below the free surface. Thus, in comparison with the torque T_∞ on the sphere,

$$\frac{T_w}{T_\infty} = \frac{Lb^2}{2a^3}.$$

For a wire diameter $2b = 0.13$ in., a length $L = 10$ in. and sphere diameter $2a = 3$ in., this yields $T_w/T_\infty \approx 10^{-4}$, which is again completely negligible compared with other sources of error.

4. Experimental procedure

Essentially the same procedure was used for both the fully and partially submerged sphere experiments. As previously indicated, the sphere was joined to the light lever via the 0.013 in. diametral wire permanently joined to the sphere. Distance from the sphere centre to the free surface was determined by means of a cathetometer. For those experiments specifically involving free-surface effects the surface level was taken as that of the bottom of the vessel-wall meniscus. Positioning of the sphere relative to the surface was achieved by raising or lowering the vessel, and hence liquid level, as required, while keeping the sphere and torque-measuring subsystem fixed.

As described earlier, careful attention was paid to temperature control to ensure the existence of isothermal conditions throughout the course of the experiments. To further ensure uniformity, after recording the initial position of the light beam and commencing vessel rotation, one hour was allowed to elapse before recording the torque. If, before the actual run, temperatures measured at any of several points lying in close proximity to the sphere deviated from one another by more than 0.1 °F, or if these temperatures changed by more than 0.1 °F over the course of the run itself, the data were discarded. Given the probable several percent inaccuracy of the viscosity data tabulated in table 1, this 0.1 °F temperature range was chosen to be consistent with that degree of accuracy.

Vessel rotation speeds varied over the range from 0.005 to 0.1 rev. s^{-1}. Angular velocities were repeatedly measured by means of a stop-watch throughout the course of each experiment to verify constancy of the vessel rotation rate. This constancy was further confirmed by monitoring the light beam for possible drift in the torque reading. Typically, successive rotation speed readings lay within 0.25% of one another.

To confirm proper functioning of all the elements entering into the experimental scheme, a careful series of 'infinite-medium' experiments were first performed. Here the sphere centre was located (approximately) at that unique point (Brenner 1964*a*) along the axis at which – correct to lowest orders in a/R_0, a/h_1 and a/h – the boundary effects engendered by the proximity of the cylinder walls and bottom to the sphere are exactly offset by the proximity of the free surface. When compared with the theoretical predictions of (1), torques measured in this mode (see figure 2) provided a high degree of confidence in the overall experimental programme.

4.1. *Data correction*

In the absence of the sphere the free surface of the rotating liquid is paraboloidal rather than flat, corresponding to the axisymmetric equation $z - z_0 = \Omega^2 R^2/2g$. Here $z - z_0$ is the height of the interface above the apex z_0 at the radial distance R from the cylinder axis, g being the acceleration due to gravity. The fluid level at the nose z_0 of this theoretically deformed surface was calculated from joint knowledge of the initial liquid level in the vessel in the absence of rotation and the known speed of rotation. The difference between these two levels was always less than 3% of the cylinder radius. Except for those runs where the sphere was almost exactly half-submerged, this difference was small compared with $|h|$. It was therefore deemed sufficient to correct for free-surface deformation only insofar as h was affected.

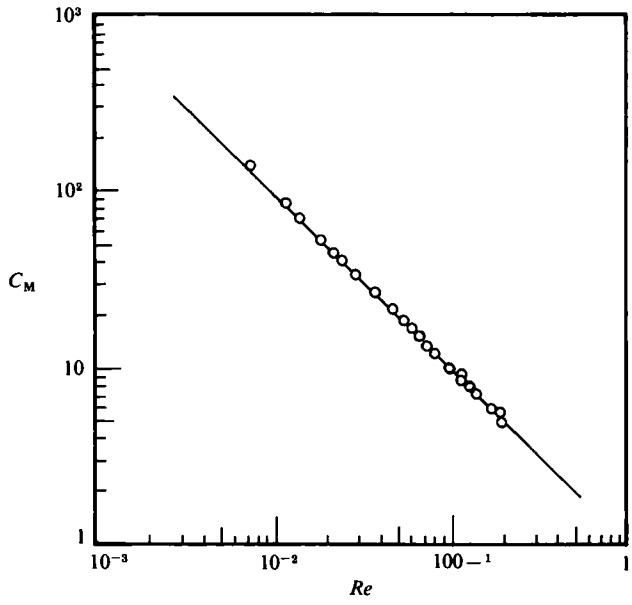

FIGURE 2. Moment coefficient $C_M = T/8\pi\rho a^5\Omega^2$ versus rotary Reynolds number $Re = a^2\Omega\rho/\mu$ in the effectively unbounded fluid. The solid line represents the theoretical Stokes-flow formula $C_M = 1/Re$. Experimental results are denoted by the circles.

Accordingly, the effective distance $|h|$ of the sphere centre O from the free surface was taken as the distance between O and the nose of the theoretical paraboloid.

Corrections arising from sphere–free–surface meniscus effects for partially penetrating spheres were estimated to be small, except perhaps in the limit where the immersed portion of the sphere was itself very small. (*A posteriori* verification of the smallness of the meniscus correction to the torque is implicitly demonstrated in figure 4. There, the measured torque is plotted against both h/a and h'/a, where h and h' are the respective distances of the sphere centre to the bulk-fluid free surface and to the top wetted circle on the circumference of the sphere, which always lay slightly above the main bulk surface of the liquid. On this same graph is also plotted for comparison the corresponding theoretical formula (4).)

5. Experimental results

Figures 2–4 summarize the results obtained.

5.1. *'Unbounded' fluid*

Define the non-dimensional rotary moment coefficient $C_M = T/8\rho a^5\Omega^2$. For the unbounded case, corresponding to (1), the theoretical value of this coefficient is

$$C_M = 1/Re, \tag{10}$$

with Re defined as before. Figure 2 is a log–log plot of measured and theoretical values of C_M versus Re. Good agreement is clearly evident, with an average deviation lying in the range 1.0–1.5% and a maximum error of about 3%.

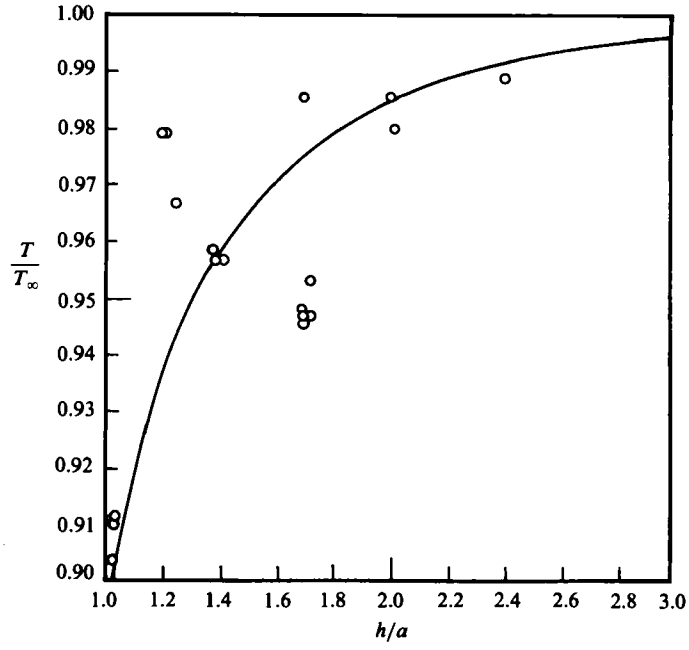

FIGURE 3. Torque on a submerged sphere in proximity to a free surface. Data points are indicated by circles. The solid curve represents the theoretical formula (2).

5.2. *Fully submerged sphere*

Figure 3 compares experimental and theoretical values of the torque ratio† T/T_∞ versus h/a for circumstances in which free-surface effects are sensible. Angular velocities varied from about 0.021–0.061 rev s^{-1}, corresponding to sphere Reynolds numbers in the range $Re = 0.03$–0.09. Again agreement between experiment and theory is satisfactory. Though the disparity may seem excessive in the case of several runs, it should be noted that the ordinate scale is greatly expanded in the plot. (A more appropriate scale for assessing the accuracy of these fully submerged sphere results is that shown in figure 5 – explicitly the range of values $1.0 \leqslant h/a \leqslant 3.0$.) Thus the average deviation is only 1.6% and the maximum error 4.4% – numbers not appreciably different from those cited in connection with figure 2. Moreover, the departures from theory do not appear systematic in algebraic sign. Especially gratifying is the excellent agreement observed for the tangent-sphere case $h/a = 1$, where free-surface penetration just begins. We are unable to explain why the maximum discrepancies in these experiments exceed, by a factor of perhaps two, those to be expected from known experimental uncertainties in viscosity, angular velocity, torsion-wire torque calibration, sphere position, etc., as well as from theoretical uncertainties – including free-surface non-planarity, centrifugal and inertial effects, wall effects, wire drag, etc.

5.3. *Partially submerged sphere*

Figure 4 shows the observed variation of the experimental torque ratio T/T_∞ with both h/a and h'/a, along with the corresponding theoretical ratio at the given h/a value. Angular velocities varied from 0.013–0.061 rev s^{-1}, corresponding to sphere

† Here, as in later figures, T is the actual experimental value, whereas T_∞ is computed from (1).

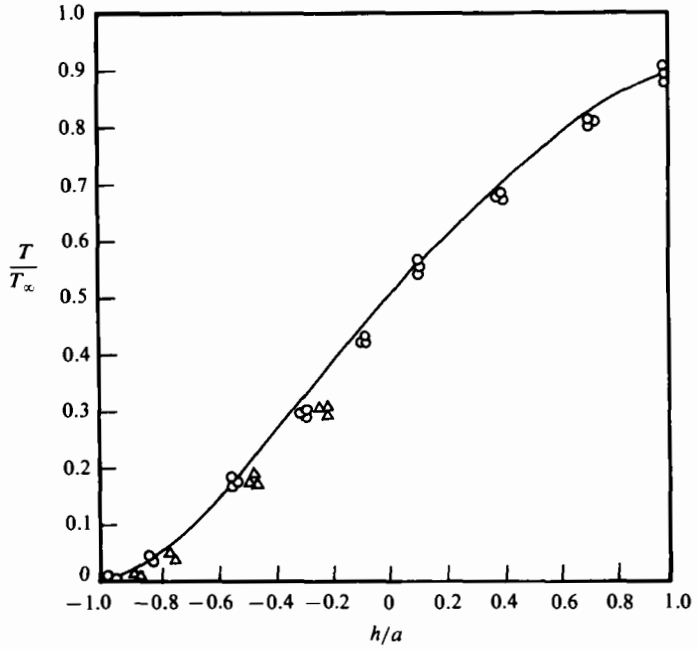

FIGURE 4. Torque on a sphere straddling a free surface. The solid curve represents the theoretical solution (4) for this case: ⊙, experimental results for the hypothetical planar free surface, namely h/a; △, experimental results for the 'top wetted point' of the sphere, h'/a.

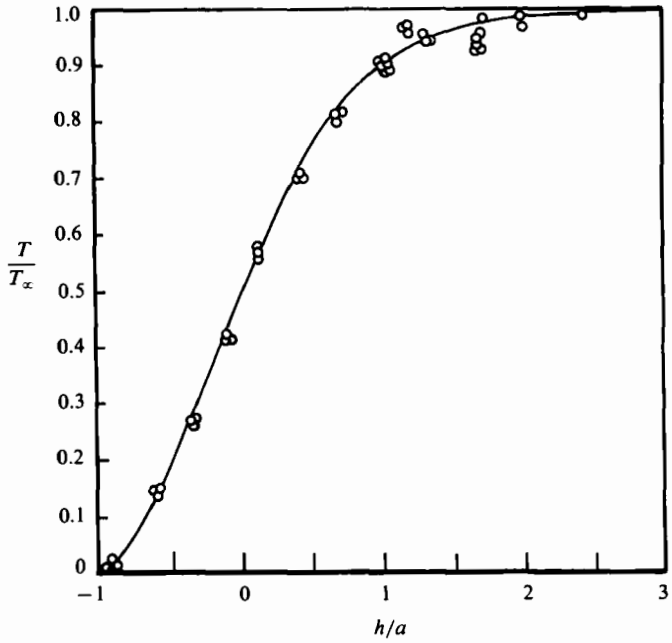

FIGURE 5. Composite of figures 3 and 4, demonstrating the continuity of the torque and its positional derivative across the tangency point $h/a = +1.0$ connecting the two different regimes.

Reynolds numbers in the range $Re = 0.02$–0.09. That the meniscus effect was indeed negligible may be inferred from the fact that better agreement between theory and experiment exists for the h/a values than for the comparable h'/a values. In any event the experiments accord quite well with the theoretical predictions of (4).

5.4. *Composite case*

Continuity of the partially and fully submerged sphere cases is illustrated in figure 5, representing a composite of figures 3 and 4 (the latter only for the hypothetical planar-free-surface case) covering the entire range ($-1.0 \leqslant h/a < \infty$) of possible degrees of sphere immersion. The experimental data are clearly consistent with the predicted continuity of both the torque ratio T/T_∞ and its derivative at the tangency point $h/a = +1.0$.

The experiments described here were performed in the Chemical Engineering Department at Carnegie–Mellon University. J.G.K. acknowledges financial support from the American Chemical Society, the Ford Foundation and the National Science Foundation. H.B. was supported by the National Science Foundation. M.E.O'N. was supported at Carnegie–Mellon University in a fellowship of Mellon Institute sponsored by the American Iron and Steel Institute. A.F. is grateful to the Chemical Engineering Department of the Massachusetts Institute of Technology for their hospitality during his sabbatical there, and to the University of Lagos for financial support.

Appendix. On the continuous variation of the torque and its derivative with sphere position

Equation (4) may be written alternatively as

$$\frac{T}{T_\infty} = \frac{\sin^3\eta_0}{2\eta_0}\int_0^\infty \left(4\frac{x^2}{\eta_0^2}+1\right)\left(1-\tanh x\tanh\frac{\pi x}{\eta_0}\right)\mathrm{d}x \tag{A 1}$$

upon setting $s = x/\eta_0$. On writing $k = 1/\eta_0$, (A 1) is equivalent to

$$\frac{T}{T_\infty} = \frac{\sin^3\eta_0}{2\eta_0} I(k), \tag{A 2}$$

with
$$I(k) = 4k^2[P+R_2(k)]+2[Q+R_0(k)], \tag{A 3}$$

where
$$P = \int_0^\infty x^2(1-\tanh x)\,\mathrm{d}x, \tag{A 4}$$

$$Q = \frac{1}{2}\int_0^\infty (1-\tanh x)\,\mathrm{d}x, \tag{A 5}$$

$$R_n(k) = \int_0^\infty \frac{x^n\tanh x\,\mathrm{e}^{-2k\pi x}}{1+\mathrm{e}^{-2k\pi x}}\,\mathrm{d}x \quad (n = 0, 2). \tag{A 6}$$

Now
$$1-\tanh x = 2[1-(1+\mathrm{e}^{-2x})^{-1}]$$
$$= 2\sum_{m=1}^{\infty}(-1)^{m+1}\exp(-2mx),$$

upon using the binomial theorem. Since

$$\int_0^\infty x^n \exp(-2mx) = \frac{n!}{(2m)^{n+1}} \quad (n = 0, 1, 2, \ldots),$$

it follows that

$$P = \frac{1}{2} \sum_{m=1}^{\infty} \frac{(-1)^{m+1}}{m^3} = \tfrac{1}{2}\eta(3), \tag{A 7}$$

$$Q = \frac{1}{2} \sum_{m=1}^{\infty} \frac{(-1)^{m+1}}{m} = \tfrac{1}{2}\eta(1), \tag{A 8}$$

where $\eta(1) = \ln 2 = 0.693147$ and $\eta(3) = 0.901543$ (Abramowitz & Stegun 1964). Furthermore,

$$\frac{e^{-2k\pi x}}{1+e^{-2k\pi x}} = 2 \sum_{m=1}^{\infty} (-1)^{m+1} \exp(-2km\pi x), \tag{A 9}$$

and, since for small $|x|$

$$\tanh x = x + O(x^3),$$

it follows from Watson's lemma (Sneddon 1951) that for $k \gg 1$

$$R_n(k) \sim \frac{2(n+1)!}{(2k\pi)^{n+2}} \sum_{m=1}^{\infty} \frac{(-1)^{m+1}}{m^{n+2}} + O(k^{-(n+4)}) \quad (n = 0, 2), \tag{A 10}$$

which gives

$$R_0(k) \sim \frac{1}{16k^2} + O(k^{-4}),$$

$$R_2(k) \sim \frac{1}{128k^4} + O(k^{-6}).$$

Consequently (A 2) yields

$$\frac{T}{T_\infty} = 2P - (P-Q)\eta_0^2 + O(\eta_0^4), \tag{A 11}$$

whence in the limit $\eta_0 = 0$ there results

$$\lim_{h/a \to 1-} \frac{T}{T_\infty} = \eta(3), \tag{A 12}$$

since $\cosh \eta_0 = h/a$. It also follows that

$$\lim_{h/a \to 1-} \left[\frac{\mathrm{d}}{\mathrm{d}(h/a)} \left(\frac{T}{T_\infty} \right) \right] = \eta(3) - \eta(1). \tag{A 13}$$

For $h/a \to 1+$ an expansion of (2) for small η_0, which may be carried out using a matched-asymptotic-expansion method similar to that of Cox & Brenner (1967*b*), yields

$$\frac{T}{T_\infty} = \eta(3) + \tfrac{1}{2}\eta_0^2 [\eta(3) - \eta(1)] + O(\eta_0^4). \tag{A 14}$$

Thus

$$\lim_{h/a \to 1-} \frac{T}{T_\infty} = \lim_{h/a \to 1+} \frac{T}{T_\infty} \tag{A 15}$$

and

$$\lim_{h/a \to 1-} \left[\frac{\mathrm{d}}{\mathrm{d}(h/a)} \left(\frac{T}{T_\infty} \right) \right] = \lim_{h/a \to 1+} \left[\frac{\mathrm{d}}{\mathrm{d}(h/a)} \left(\frac{T}{T_\infty} \right) \right], \tag{A 16}$$

showing that the torque is both continuous and differentiable at $h/a = 1$, i.e. as the sphere penetrates the free surface.

REFERENCES

ABRAMOWITZ, M. & STEGUN, I. A. 1964 *Handbook of Mathematical Functions*, pp. 803–811. U.S. National Bureau of Standards.

ASHARE, E., BIRD, R. B. & LESCARBOURA, J. A. 1965 Falling-cylinder viscometers for non-Newtonian fluids. *AIChE J.* **11**, 910–916.

BERDAN, C. & LEAL, L. G. 1984 Motion of a sphere in the presence of a deformable interface. Part 3. An experimental study of translation normal to the interface. *J. Coll. Interface Sci.* (in press).

BOWDEN, F. P. & LORD, R. G. 1963 The aerodynamic resistance to a sphere rotating at high speed. *Proc. R. Soc. Lond.* A **271**, 143–153.

BRENNER, H. 1961 The slow motion of a sphere through a viscous fluid towards a plane surface. *Chem. Engng Sci.* **16**, 242–251.

BRENNER, H. 1964*a* Slow viscous rotation of an axisymmetric body in a circular cylinder of finite length. *Appl. Sci. Res.* A**13**, 81–120.

BRENNER, H. 1964*b* The Stokes resistance of an arbitrary particle II. An extension. *Chem. Engng Sci.* **19**, 599–629.

BRENNER, H. & LEAL, L. G. 1978 A micromechanical derivation of Fick's law for interfacial diffusion of surfactant molecules. *J. Colloid Interface Sci.* **65**, 191–209.

BRENNER, H. & LEAL, L. G. 1982 Conservation and constitutive equations for adsorbed species undergoing surface diffusion and convection at a fluid–fluid interface. *J. Colloid Interface Sci.* **88**, 136–184.

CASWELL, B. 1970 Effect of finite boundaries on the motion of particles in non-Newtonian fluids. *Chem. Engng Sci.* **25**, 1167–1176.

CHILDRESS S. 1964 The slow motion of a sphere in a rotating viscous fluid. *J. Fluid Mech.* **20**, 305–314.

CHO, Y. I. & HARTNETT, J. P. 1979 Falling ball viscometer – a new instrument for viscoelastic fluids. *Lett. Heat Mass Transfer* **6**, 335–342.

COX, R. G. & BRENNER, H. 1967*a* Effect of finite boundaries on the Stokes resistance of an arbitrary particle. Part 3. Translation and rotation. *J. Fluid Mech.* **28**, 391–411.

COX, R. G. & BRENNER, H. 1967*b* The slow motion of a sphere through a viscous fluid towards a plane surface. II. Small gap widths, including inertial effects. *Chem. Engng Sci.* **22**, 1753–1777.

DAVIS, A. M. J. & O'NEILL, M. E. 1979 Slow rotation of a sphere submerged in a fluid with a surfactant surface layer. *Intl J. Multiphase Flow* **5**, 413–425.

DAVIS, P. K. 1965 Motion of a sphere in a rotating fluid at low Reynolds number. *Phys. Fluids* **8**, 560–567.

DENNIS, S. C. R. & INGHAM, D. B. 1982 The boundary layer on a fixed sphere on the axis of an unbounded viscous fluid. *J. Fluid Mech.* **123**, 210–236.

DENNIS, S. C. R., INGHAM, D. B. & SINGH, S. N. 1982 The slow translation of a sphere in a rotating fluid. *J. Fluid Mech.* **117**, 251–267.

DENNIS, S. C. R., SINGH, S. N. & INGHAM, D. B. 1980 The steady flow due to a rotating sphere at low and moderate Reynolds numbers. *J. Fluid Mech.* **101**, 257–279.

FALADE, A. 1982 Arbitrary motion of an elliptic disk at a fluid interface. *Intl J. Multiphase Flow* **8**, 543–551.

FLUIDE, M. J. C. & DABORN, J. E. 1982 Viscosity measurement by means of falling spheres compared with capillary viscometry. *J. Phys.* E: *Sci. Instrum.* **15**, 1313–1321.

GEILS, R. H. 1977 Small-volume inclined falling-ball viscometer. *Rev. Sci. Instrum.* **48**, 783–785.

HIRSCHFELD, B. R., BRENNER, H. & FALADE, A. 1984 First- and second-order wall effects upon the slow viscous asymmetric motion of an arbitrarily-shaped, -positioned and -oriented particle within a circular cylinder. *Physicochem. Hydrodyn.* **5**, 99–133.

HOCKING, L. M., MOORE, D. W. & WALTON, I. C. 1979 Drag on a sphere moving axially in a long rotating cylinder. *J. Fluid Mech.* **90**, 781–793.

JEFFERY, G. B. 1915 On the steady rotation of a solid of revolution in a viscous fluid. *Proc. Lond. Math. Soc.* **14**, 327–338.

KUNESH, J. G. 1971 Experiments on the hydrodynamic resistance of translating–rotating particles. Ph.D. thesis, Carnegie–Mellon University.

LAMB, H. 1932 *Hydrodynamics*, 6th edn, p. 585. Cambridge University Press.

LEAL, L. G. & LEE, S. H. 1982 Particle motion near a deformable fluid interface. *Adv. Coll. Interface Sci.* **17**, 61–81.

MAJUMDAR, S. R., O'NEILL, M. E. & BRENNER, H. 1974 Note on the slow rotation of a concave spherical lens or bowl in two immiscible semi-infinite viscous fluids. *Mathematika* **21**, 147–154.

MAXWORTHY, T. 1965 An experimental determination of the slow motion of a sphere in a viscous rotating fluid. *J. Fluid Mech.* **23**, 373–384.

MAXWORTHY, T. 1970 The flow created by a sphere moving along the axis of a rotating slightly-viscous fluid. *J. Fluid Mech.* **40**, 453–479.

MENA, B., LEVINSON, E. & CASWELL, B. 1972 Torque on a sphere inside a rotating cylinder. *Z. angew. Math. Phys.* **23**, 173–181.

MUNRO, R. G., PIERMARINI, G. J. & BLOCK, S. 1979 Wall effects in diamond-anvil pressure-cell falling-sphere viscometers. *J. Appl. Phys.* **50**, 3180–3184.

O'NEILL, M. E. & RANGER, K. B. 1979 On the rotation of a rotlet or sphere in the presence of an interface. *Intl J. Multiphase Flow* **5**, 143–148.

RANGER, K. B. 1978 Circular disk straddling the interface of two-phase flow. *Intl J. Multiphase Flow* **4**, 263–277.

RICHARDSON, P. D. 1976 Flow beyond an isolated rotating disk. *Intl J. Heat Mass Transfer* **19**, 1189–1195.

SAWATZKI, O. 1970 Flow field around a rotating sphere. *Acta Mech.* **9**, 159–214.

SCHNEIDER, J. C., O'NEILL, M. E. & BRENNER, H. 1973 On the slow viscous rotation of a body straddling the interface between two immiscible semi-infinite fluids. *Mathematika* **20**, 175–196.

SNEDDON, I. N. 1951 *Fourier Transforms*, p. 516. McGraw-Hill.

SONSHINE, R. M., COX, R. G. & BRENNER, H. 1966 The Stokes translation of a particle of arbitrary shape along the axis of a circular cylinder filled to a finite depth with viscous liquid. *Appl. Sci. Res.* **16**, 273–300; 325–360.

TAYLOR, G. I. 1923 The motion of a sphere in a rotating liquid. *Proc. R. Soc. Lond.* A **102**, 180–189.

THOMAS, R. H. & WALTERS, K. 1964 Motion of elasto–viscous fluid due to sphere rotating about its diameter. *Q. J. Mech. Appl. Maths* **17**, 39–53.

WALTERS, K. & WATERS, N. D. 1963 On the use of a rotating sphere in the measurement of elasto-viscous parameters. *Brit. J. Appl. Phys.* **14**, 667–671.

WATERS, N. D. & GOODEN, D. K. 1980 Couple on a rotating oblate spheroid in an elasto-viscous fluid. *Q. J. Mech. Appl. Maths* **33**, 189–206.

WEIN, O. 1979 Rotational quasi-viscometric flows around a rotating sphere. *J. Non-Newtonian Fluid Mech.* **5**, 297–313.